

Aalborg Universitet



AALBORG  
UNIVERSITY

## Optimal Probabilistic Planning of Passive Harmonic Filters in Distribution Networks with High Penetration of Photovoltaic Generation

Jannesar, Mohammad Rasol ; Sedighi, Alireza; Savaghebi, Mehdi; Anvari-Moghaddam, Amjad ; Guerrero, Josep M.

*Published in:*  
International Journal of Electrical Power & Energy Systems

*DOI (link to publication from Publisher):*  
[10.1016/j.ijepes.2019.03.025](https://doi.org/10.1016/j.ijepes.2019.03.025)

*Creative Commons License*  
CC BY-NC-ND 4.0

*Publication date:*  
2019

*Document Version*  
Accepted author manuscript, peer reviewed version

[Link to publication from Aalborg University](#)

*Citation for published version (APA):*  
Jannesar, M. R., Sedighi, A., Savaghebi, M., Anvari-Moghaddam, A., & Guerrero, J. M. (2019). Optimal Probabilistic Planning of Passive Harmonic Filters in Distribution Networks with High Penetration of Photovoltaic Generation. *International Journal of Electrical Power & Energy Systems*, 110, 332-348. <https://doi.org/10.1016/j.ijepes.2019.03.025>

### General rights

Copyright and moral rights for the publications made accessible in the public portal are retained by the authors and/or other copyright owners and it is a condition of accessing publications that users recognise and abide by the legal requirements associated with these rights.

- Users may download and print one copy of any publication from the public portal for the purpose of private study or research.
- You may not further distribute the material or use it for any profit-making activity or commercial gain
- You may freely distribute the URL identifying the publication in the public portal -

### Take down policy

If you believe that this document breaches copyright please contact us at [vbn@aub.aau.dk](mailto:vbn@aub.aau.dk) providing details, and we will remove access to the work immediately and investigate your claim.



# Optimal Probabilistic Planning of Passive Harmonic Filters in Distribution Networks with High Penetration of Photovoltaic Generation

Mohammad Rasol Jannesar, Alireza Sedighi\*, Mehdi Savaghebi, Amjad Anvari-Moghaddam, and Josep M. Guerrero

**Abstract**--In recent years, distribution networks have been increasingly affected by the random nature of harmonic sources introduced by nonlinear load and renewable energy sources (RES) such as photovoltaic (PV) systems. This paper presents an approach based on Genetic Algorithm (GA) and Monte-Carlo Simulation (MCS) for the optimal planning of single-tuned passive harmonic filters (PHFs) in a distribution network. The resistance and inductance of the lines within the network are modeled by frequency dependent characteristics. The probabilistic characteristics of the load and PV system currents are also considered for optimal planning of PHFs. In our optimization model, the objective function minimizes the total PHF installation cost and the energy losses, by considering the total harmonic distortion (THD) of bus voltages and maximum capacity of PHF as constraints. The proposed method is validated by a simulation study using an unbalanced three-phase real distribution system. An advantage of this method over most of the conventional approaches is that both harmonic current magnitude and phase angle of real PV systems are taken into account. Numerical results show the applicability and effectiveness of the proposed method.

**Index Terms**--harmonic mitigation, high photovoltaic penetration, passive harmonic filter, probabilistic planning.

## I. INTRODUCTION

Harmonic problems arising from the power electronic-based devices and nonlinear loads are increasing in distribution networks. On the other hand, penetration of renewable energy sources (RES), especially photovoltaic (PV) systems [1] with power electronic converters is continuously increasing [2]. Due to increasing harmonic currents of nonlinear loads and PV systems, total harmonic distortion of voltage ( $THD_v$ ) is increasing. In addition, energy losses [3] and the risk of resonance phenomenon [4] may elevate by installing PV systems. Harmonic currents produced by nonlinear loads and PV systems are unpredictable mainly due to different consumers' energy consumption patterns and intermittent shading (due to changing weather conditions caused by clouds, storms, rain, etc.), respectively [5]. Therefore, probabilistic methods should be applied for harmonic analyses [6]. Optimal filter planning is one of the solutions to mitigate harmonic problems [7]. Passive harmonic filters (PHFs) are divided into series, shunt, and series-shunt types. Series and shunt filters mitigate harmonic current in specific order(s) by providing high and low impedance paths, respectively [8]. In addition, active harmonic filters produce proper harmonic currents to decrease

---

\*: corresponding author: Department of Electrical Engineering, Yazd University, University Blvd, Safayieh, Yazd, Iran, P.C.: 89158-18411.

Declarations of interest: none

M. R. Jannesar and A. Sedighi are with Department of Electrical Engineering, Yazd University, Yazd, Iran (e-mail: mohammadrasol@gmail.com; sedighi@yazd.ac.ir).

M. Savaghebi is with Electrical Engineering Section, Mads Clausen Institute, University of Southern Denmark, Odense, Denmark (e-mail: mesa@mci.sdu.dk)

A. Anvari-Moghaddam, and Josep M. Guerrero are with Department of Energy Technology, Aalborg University, Aalborg, Denmark (e-mail: aam@et.aau.dk; joz@et.aau.dk).

THD<sub>v</sub> [9]. The PHFs are still widely used in power systems due to simplicity and low cost [10]. Single-tuned is the most popular, efficient, and economical type of shunt PHFs [11]. Although in many works, angles of harmonic orders are neglected in harmonic analyses, it is important to consider both magnitude and angle of harmonic currents injected in case of high nonlinear loads and PV systems penetration. By considering the angles of harmonic currents, some harmonic components may cancel out each other. Therefore, the optimal capacity of PHF may be decreased. The IEEE Standard 519-2014 provides a guideline for the limitation and mitigation of harmonics.

Many studies on optimal PHF planning have been conducted in the literature that can be divided to deterministic and probabilistic methods. For instance, authors of [12, 13, 14] applied deterministic methods to simultaneously minimize the investment cost, total harmonic distortion of current (THD<sub>I</sub>) and THD<sub>v</sub> of the system buses through a multi-objective filter planning optimization model. However, system losses are neglected in this process. In [15], several objective functions are considered as performance indices in the filter-planning problem but optimal placement and sizing are not performed simultaneously. In [16], minimization of power losses and investment cost of PHFs are considered as the objectives of the optimal planning problem. Voltage limits, number/size of installed PHFs, location of PHFs installation and THD<sub>v</sub> of all buses are taken into account as constraints. In [17], optimal planning of distributed generation (DG) is added to the objective function of [16] and is simultaneously solved with planning of PHF. Authors of [18] propose the optimal sizing of single-tuned filters to maximize power factor (PF) and transmission efficiency while minimizing energy loss; however, PHF cost is not taken into account. In another study, a multi-objective planning of PHFs and capacitors is performed to decrease PHF cost, energy losses as well as voltage distortion and deviation [19]. In [20, 21], an optimal multi-objective design method (without optimal placement) is proposed for different types of PHFs based on the modified Bat algorithm and Pareto front to minimize power loss, THD<sub>v</sub>, and THD<sub>I</sub>. In a number of research works, the optimal design of PHF is proposed for increasing the loading of distribution/service transformers. For instance, in [22], comparative evaluation of PHFs is proposed to minimize harmonic loss factor (F<sub>HL</sub>), THD<sub>v</sub>, THD<sub>I</sub>, and displacement power factor (DPF). In [23], an optimal passive filter design approach is provided to maximize the power factor considering frequency-dependent line losses, under the harmonically contaminated voltages and currents. Optimal filter parameters are also calculated in [24] using different optimization algorithms to maximize the suggested power factor function.

However, in many cases, harmonic currents caused by nonlinear loads and PVs have a probabilistic nature. For example, in [25], a linear approximation method and a chance-constrained programming model are presented for optimal planning of single-tuned PHFs in an industrial network. The objective is to minimize the total filter installation cost, while harmonic current limits and filter component constraints are satisfied with predetermined confidence levels. However, energy losses and optimal sitting of PHFs are not considered in the objective function. The authors of [26] present a new method considering the probabilistic characteristics of harmonic current sources for planning of single-tuned PHFs in a power system. The objective is to minimize the voltage distortion throughout the system while determining the optimal filter locations and sizes. However, PHF cost and energy losses are not taken into account in that work. In [27], the disadvantages of [25] and [26] are covered without considering the energy losses.

In [28], a simplified heuristic approach is proposed for PHF planning to improve power quality indices and minimize the total costs of filter and losses. In the same work, both deterministic and uncertain frameworks are taken into account.

In [29], a new method for studying PHFs planning using Simultaneous Perturbation Stochastic Approximation (SPSA) is presented and the optimal number, placement, and sizing of PHFs are calculated. However, only PHF cost is included in the objective function and reduction of energy losses is not taken into account. The objective function and constraints of [30] are very similar to those of [29], but, in [30] three load levels are considered for load modeling and an Adaptive Dynamic Clone Selection Algorithm (ADCSA) is applied for optimization. However, reduction of energy losses is not considered in [30].

In [10], multiple scenarios including different load levels and harmonic currents are studied for PHF planning. However, similar to [30], energy losses are not modeled in the objective function. Authors of [31] present an approach of combining Feasible-Direction Method and a Genetic Algorithm (FDM+GA) to investigate the planning of PHFs. However, the optimal placement of PHF is not determined in planning approach. In [32], optimal multi-objective planning of PHFs using Hybrid Differential Evolution (HDE) method is investigated. Objective function is defined under three loading levels, but, optimal placement and sizing of PHFs is not computed. Likewise, in [33], a methodology is presented for probabilistic harmonic resonance assessment considering power system uncertainties. This approach uses both Monte-Carlo Simulation (MCS) and harmonic resonance mode analysis techniques.

Authors of [34] presented a method for planning PHFs, based on combining Sequential Neural-network Approximation and Orthogonal Arrays (SNAOA). In the objective function, the impacts of  $THD_v$  and  $THD_i$  are considered, but, energy losses and PHF cost are not taken into account. In [35], PHF cost is modeled to tackle the shortcoming of [34], but, still energy losses are not included in the optimization.

A scheme for mitigating harmonic problems in distribution systems is presented in [36] by deploying multiple low-cost distributed plug-in active filters and using MCS-based probabilistic harmonic power flow method.

In [37], optimal designing of single-tuned PHFs corresponding to the minimum power losses is addressed. However, optimal PHFs placement and cost are not considered. Authors of [38] formulate the planning problem of PHFs as a probabilistic multi-objective optimization problem by using a heuristic approach. In [38], the objective function consists of PHF installation cost, probabilistic  $THD_v$ , and fundamental voltage index. However, the candidate buses for PHF installation are limited and energy losses are not included in the optimization. Optimal probabilistic planning of PHFs is presented in [39] by considering  $THD_v$  limits and filter capacity as constraints. In the same work, PHFs investment cost and imaginary parts of the harmonic currents are considered, but, energy losses are not taken into account. Authors of [40] present an optimal planning approach for PHFs using the HDE method and considering variations of system impedance, harmonic current sources, and filter tuning frequency. However, investment cost of filter and energy losses are not considered. In [41], the application of PHF at the hybrid renewable microgrid has addressed to reduce  $THD_v$  and PHF cost taken into account uncertainties of RES.

In the present paper, optimal probabilistic PHF placement and sizing are performed simultaneously by considering nonlinear loads and high PV penetration to minimize  $THD_v$ , PHFs cost, and energy losses.  $THD_v$  of buses and maximum capacity of filter are considered as constraints. In addition, unlike most of the reviewed literature, both magnitude and phase angle of harmonic currents are included in our stochastic studies for PHF planning. To do so, PV harmonic currents are measured by a power analyzer for one week for a single-phase PV system in a real distribution network. Then, by using distribution fitting techniques, the Probabilistic Distribution Function (PDF) of PV magnitudes and phase angles are calculated for harmonic orders 1st to 25th. Probabilistic harmonic power flow is also performed by MCS. Inverse-transform method is considered for random variable generation. Additionally, the PDF of load is assumed as a normal PDF. Finally, the resistance and inductance of lines within the examined distribution network are modeled by frequency dependent characteristics.

The rest of this paper is structured as follows: in Section II, the modeling of filter and distribution network is introduced. Also, probabilistic harmonic load flow and calculation method for PDF of PV current magnitude and phase angle are discussed. Cost function and the methods for optimization are explained in Section III. In Section IV, computer simulations and numerical results are presented and analyzed. Finally, Section V concludes the paper with a brief summary.

## II. SYSTEM MODELING

### A. Filter Modeling

PHFs are divided into three groups including series, shunt, and series-shunt. The most common type of PHF is the single-tuned (notch) filter. In the present paper, this filter type is used to mitigate harmonic effects of nonlinear loads and PV systems due to its low cost and high efficiency. The notch filter presents a low impedance in a specific harmonic current and connects in shunt with the power system (Fig. 1). In addition to harmonic mitigation, notch filters can provide power factor correction.

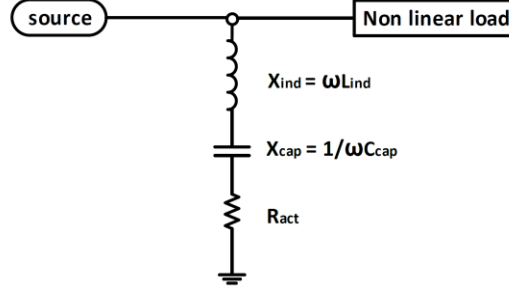


Fig. 1. Single-tuned filter

In notch filters, harmonic tuning order ( $n_{res}$ ) can be calculated as

$$n_{res} = \frac{f_{res}}{f_1} \quad (1)$$

where  $f_{res}$  and  $f_1$  are resonance and nominal frequencies, respectively.

The three-phase rated capacitive power ( $Q_{cap}$ ) of capacitance and reactive power ( $Q_{ind}$ ) of inductance can be calculated according to the following equations [42] (see Appendix section for more information). In addition, three-phase RMS values for reactive powers of capacitance ( $Q_{rms\,cap}$ ) and inductance ( $Q_{rms\,ind}$ ) are calculated according to the following equations

$$\begin{aligned} Q_{cap} &= Q_{tot} \cdot \left(1 - \frac{1}{n_{res}^2}\right) & , & & Q_{rms\,cap} &= 3 \times \sqrt{\sum_{i=1} (V_{i\,cap})^2} \times \sqrt{\sum_{i=1} (I_i)^2} \\ Q_{ind} &= Q_{tot} \cdot (n_{res}^2 - 1) & , & & Q_{rms\,ind} &= 3 \times \sqrt{\sum_{i=1} (V_{i\,ind})^2} \times \sqrt{\sum_{i=1} (I_i)^2} \end{aligned} \quad (2)$$

where  $Q_{tot}$  is the three-phase rated reactive power of a single-tuned filter.  $V_{i\,cap}$  and  $V_{i\,ind}$  represent  $i^{\text{th}}$  order harmonic of voltage across capacitor and inductor, respectively.  $I_i$  is  $i^{\text{th}}$  order of filter current.

PHF power loss can be calculated by the following equations

$$X_{ind} = \frac{U_1^2}{Q_{ind}} \rightarrow R_{act} = \frac{X_{ind}}{Q_f} \rightarrow I_1 = \frac{Q_{tot}}{\sqrt{3} \times U_1} \rightarrow P_{act} = 3 \times R_{act} \times I_1^2 \quad (3)$$

where  $X_{ind}$  is the inductive reactance for one phase,  $U_1$  is nominal line-line voltage,  $R_{act}$  is resistance of PHF,  $Q_f$  is quality factor,  $I_1$  is nominal current magnitude, and  $P_{act}$  is power loss of PHF.

### B. Distribution Line Modeling

Due to the skin effect, the internal conductor inductance decreases because of less internal flux linkages and the resistance increases because the effective cross-sectional area decreases [43]. Frequency polynomial characteristic can be defined as (4) for modeling frequency-dependent behavior of power lines.

$$y(f_h) = \left( (1-a) + a \times \left( \frac{f_h}{f_1} \right)^b \right) \times y(f_1) \quad (4)$$

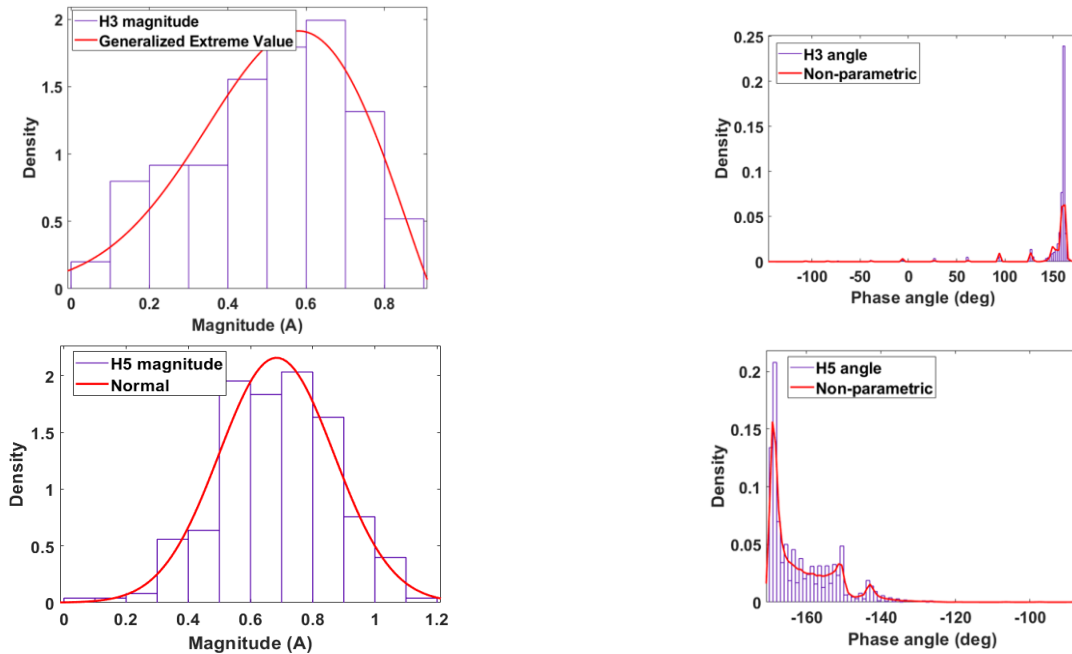
where  $y(f_h)$  and  $y(f_1)$  represent resistance or inductance for  $h^{\text{th}}$  and first order harmonics, respectively.  $a$  and  $b$  are parameters specifying the degree of frequency dependence. This model is used for cables and transformers, while, low voltage (LV) overhead lines are modeled by a tower type of DIgSILENT that considers frequency dependence of lines automatically. To do this, the parameters such as DC-resistance, geometrical mean radius (GMR), outer diameter, and distance between overhead and ground lines are set in DIgSILENT. Values of  $a$  and  $b$  are obtained from DIgSILENT Library and shown in Table I. These values are selected according to voltage level of cables and transformer.

TABLE I  
Values of  $a$  and  $b$  for cables and transformer

Equipment	Resistance	Inductance
Cables	$a=0.1 ; b=0.9$	$a=1 ; b=-0.65$
Transformer	$a=0.2 ; b=1.5$	$a=1 ; b=-0.03$

### C. Probabilistic Distribution Functions of Load and PV Harmonic

THD<sub>I</sub> of PV system increases when the power production decreases or THD<sub>V</sub> of PV bus increases [44]. Due to the random nature of the irradiance, PV harmonics are probabilistic and thus, can be modeled by PDF [45, 46, 47, 48]. To represent the harmonic behavior of grid-connected PVs, harmonic current magnitudes and angles of a PV farm are measured initially by a power analyzer within one week in an unbalanced three-phase real distribution system. Then, the best probabilistic distribution function is recognized for different harmonic orders using distribution fitting feature in MATLAB. Based on this, it is possible to display the fitted distribution over plots of PDF, cumulative distribution function (CDF), probability plots, and survivor functions. Also, two or more traditional PDFs and non-parametric functions can be fitted by comparing the results, and select the most valid model. In Fig. 2, some best PDF fittings of harmonic current magnitude and angle of the studied PV are shown.



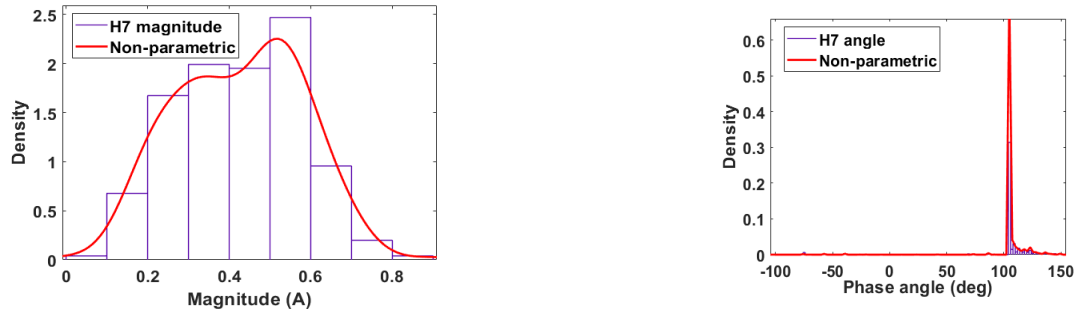


Fig. 2. Best PDF fittings of harmonic current magnitude and angle for 3<sup>rd</sup>, 5<sup>th</sup>, and 7<sup>th</sup> orders

After specifying the most valid PDF for harmonic current magnitude and phase angle in any order (e.g. normal and non-parametric PDF for 5<sup>th</sup> order harmonic current magnitude and angle, respectively), the inverse CDF is calculated. As explained in the MCS, there are various general methods for generating one-dimensional random variables from a prescribed distribution. In the present paper, the inverse-transform method is considered for random variable generation to increase the convergence rate of MCS. The random variable can be calculated as

$$X = F^{-1}(U) \quad (5)$$

where  $U$  is the uniform distribution,  $F^{-1}$  is inverse CDF, and  $X$  is random variable. Fig. 3 shows the concept of this method [49].

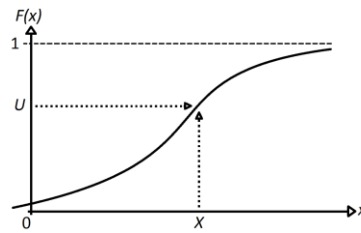


Fig. 3. Inverse-transform method

Considering the central limit theorem, the annual average for residential load distribution can be represented by a normal distribution function even if the individual daily loads are not normally distributed. Such assumption has also been made in numerous research works where a normal distribution function is applied for residential loads in distribution systems (e.g. [48, 50]). Standard deviation is assumed not very large (equal to 20%) to decrease the variation of load; and thus guarantee the worst case of  $THD_v$ . Fig. 4 shows the mean value for load harmonic current magnitude and phase angle calculated according to [51].

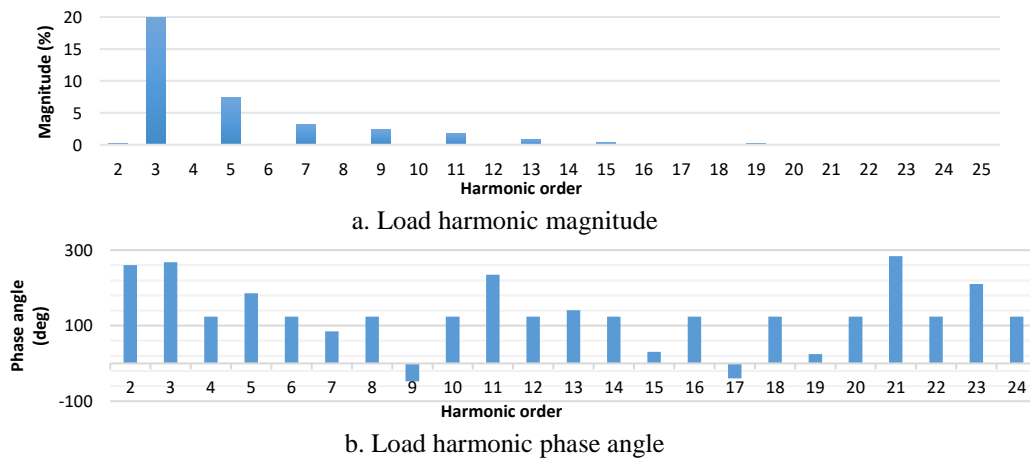


Fig. 4. Load harmonic current

#### D. Probabilistic Harmonic Load Flow by MCS

Since PV generation and load are mostly uncertain, probabilistic studies should be carried out. In order to handle the probabilistic load flow problem, some approaches have been studied in the literature. The proposed procedures could be divided into MCS-based, analytical, and approximate methods [52].

MCS is an iterative method to solve the probabilistic problem. In this approach, first of all, sufficient numbers of samples should be generated. There are various general methods for generating one-dimensional random variables from a prescribed distribution including inverse-transform, Alias, composition, acceptance-rejection, etc. [49]. As already mentioned, the inverse-transform method is considered in the present work for random variable generation.

Unbalanced harmonic load flow is performed in DIGSILENT. In this regard, harmonics of loads and PVs are modeled as current source including magnitude and angle for orders 1 to 25. For the nodes that contain both load and PV, the total harmonic current can be calculated using Kirchhoff's Current Law in each order. In the harmonic load flow calculation, a steady-state network analysis is carried out at each frequency at which harmonic sources are defined.

THD<sub>v</sub> of buses can be calculated by harmonic load flow and the generated samples of harmonic current sources. Calculating THD<sub>v</sub> is continued until maximum sample number of MCS is reached. As a result, the PDF of variables such as THD<sub>v</sub> and energy losses are provided.

### III. OBJECTIVE FUNCTION AND SOLVING METHOD

The objective function that should be maximized is defined as (6) based on net present value:

$$\text{maximize: } \left\{ \sum_{L=1}^N \left[ B_{LOSS} \times \left( \frac{1+ir}{1+dr} \right)^L \right] - C_{PHF} \right\} \quad (6)$$

where  $B_{LOSS}$  is benefit of loss reduction,  $C_{PHF}$  is PHF investment cost,  $ir$  and  $dr$  are inflation and discount rates, and  $N$  is the number of operation years. Since the benefit of loss reduction is realized during the planning and operation horizon, its value is multiplied by  $\left( \frac{1+ir}{1+dr} \right)^L$  to calculate the present value. Benefit of loss reduction is defined as:

$$B_{LOSS} = \frac{1}{M} \left( \sum_{S=1}^M (LOSS_{old})_S - (LOSS_{new})_S \right) \times Pr_m \times 24 \times 360 \quad (7)$$

where  $S$  and  $M$  are generated samples and the maximum sample number of MCS, respectively.  $(LOSS_{old})_S$  and  $(LOSS_{new})_S$  are losses for generated sample  $S$  before and after PHF planning, respectively. Therefore, the expected value of loss reduction is calculated in (7). Also,  $Pr_m$  is the average daily energy price. The hourly benefit is multiplied by 24 to calculate daily benefit and daily benefit is multiplied by 360 to calculate annual benefit.

PHF investment cost [53] can be defined as

$$C_{PHF} = (C_{act} \times P_{act}) + (C_{fix_{cap}} + C_{cap} \times Q_{rms_{cap}}) + (C_{ind} \times Q_{rms_{ind}}) \quad (8)$$

where  $C_{act}$  is the PHF resistance cost and  $C_{fix_{cap}}$  is fixed cost of capacitor installation. Also,  $C_{cap}$  and  $C_{ind}$  are the PHF capacitor and inductor costs, respectively.

Constraints consist of THD<sub>v</sub>, RMS voltage limit, and PHF component limit. THD<sub>v</sub> constraint can be defined as:

$$P\{THD_{v,i} \leq THD_{v,max}\} > C ; \quad \forall i \in N_b \quad (9)$$

where  $THD_{v,max}$  is the maximum allowed THD<sub>v</sub> at any node  $i$  within the studied network with  $N_b$  nodes and  $P\{\cdot\}$  denotes the probability of event  $\{\cdot\}$ . Also,  $C$  is the confidence or limit level of the allowable probability that is assumed to be 95% in this paper [54]. According to [8] and IEEE Standard 1159-2009, the utilization

voltage is permitted to be in the range of -10 to +10 percent of the nominal voltage. As the PHF component constraint, maximum rated reactive power of PHF is limited to 127 kVAr.

Fig. 5 shows the flowchart of the solution methodology. Firstly, modeling of cables, transformers, and overhead lines is performed to consider frequency dependence of distribution line. Also, PDF and inverse CDF of PVs are calculated by distribution fitting techniques introduced in Section II-C. In the next step, maximum iterations for GA and number of generated samples for MCS are assumed equal to 30 and 100 respectively. Also, the initial generation of GA is created. The format of the gene is shown in Fig. 6. The population size of GA is 200. The range of PHF number, tuning order, rated reactive power, and PHF placement are between 1 to 7, 2 to 15, 1 to 127 (kVAr), and 0 to 31, respectively.

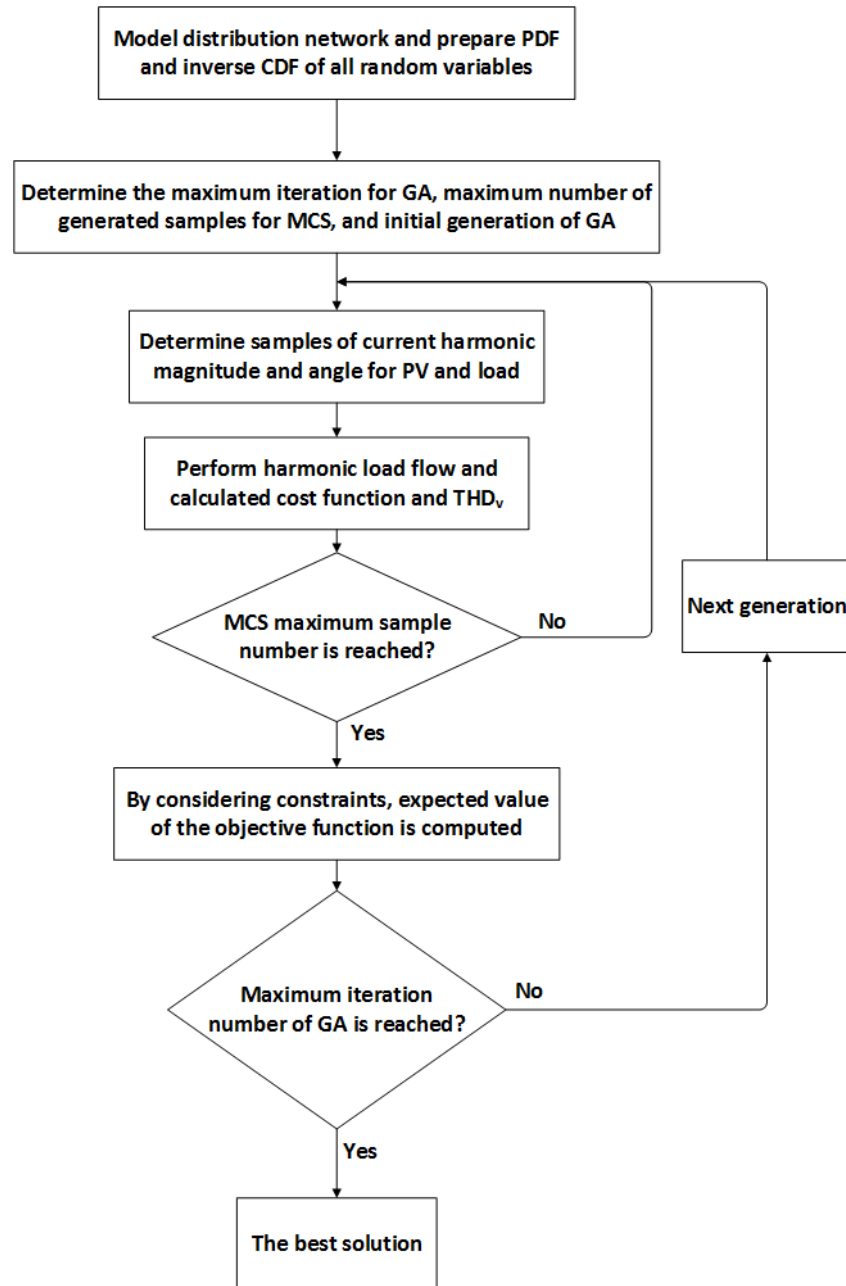


Fig. 5. Flowchart of the solution methodology

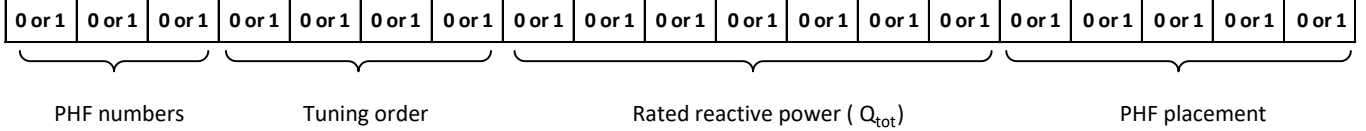


Fig. 6. The gene's representation

The number of PHFs is optimized by GA. According to Fig. 6, when the number of PHFs is for instance equal to 4 in a generation of GA, the number of genes is equal to 67 (3 genes for PHF number,  $(4 \times 4)$  genes for tuning order,  $(4 \times 7)$  genes for rated reactive power, and  $(4 \times 5)$  genes for PHF placement). In other words, for each PHF, a string containing 16 genes (4 genes for tuning order, 7 genes for rated reactive power, and 5 genes for PHF placement) is added to the number of genes. In general, the PHF number is the number of PHFs that are placed in different places by different rated reactive powers and tuning orders (1 PHF in each place).

In the third step, samples of harmonic current magnitude and angle for PVs are determined by inverse-transform method introduced in Section II-C. To calculate samples of nonlinear loads, a stochastic number is generated according to a normal distribution function. In the next step, unbalanced harmonic load flow is performed by considering load and PV harmonics. Then energy losses,  $\text{THD}_v$ , and thus, value of cost function are evaluated. In the fifth step, the stop criterion for scenario making by MCS is checked.

In the sixth step, if the  $\text{THD}_v$  constraint is not violated, the expected value of the objective function is calculated for the current generation. Then, the stop criterion for the outer loop (which counts the number of GA iterations) is checked. If the maximum number of iterations is reached, the best solution that has the maximum loss reduction and minimum PHF cost is recognized and printed.

#### IV. NUMERICAL RESULT

As demonstrated in Fig. 7, the case study system is a 383-buses real LV distribution system located in Yazd province, Iran.

This system is connected to a 20 kV system by a 20 kV / 0.4 kV transformer while feeding 299 nonlinear residential loads. This network is feeding two main feeders that can be divided into upstream (above) and downstream (below) the transformer. In the sub system below the transformer, two single-phase PV systems labeled as PV1 and PV2, each with the capacity of 5 kW, are located at the end of the feeder connected between phase A and neutral. By considering PV1 and PV2, total active and reactive loads of the feeder below transformer are 141 kW and 64 kVAr, respectively. When no PVs are connected to the network, the maximum active and reactive powers of phase A, B and C are almost equal to 50 kW and 21 kVAr, respectively. Therefore, penetration of PVs located in the real network is equal to 20%. In simulations, the penetration of PVs is initially increased to 50 % by adding 5 kW PVs to buses T525, T660, and T531. Then, the penetration of PVs reaches 80% (which is regarded here as a high penetration rate) by adding 5 kW PVs to buses T529, T533, and T538. PV nodes for each penetration are summarized in Table II.

TABLE II  
PV nodes for each penetration

Penetration (%)	PV nodes
20	T379 and T371
50	T379, T371, T525, T660, and T531
80	T379, T371, T525, T660, T531, T529, T533, and T538

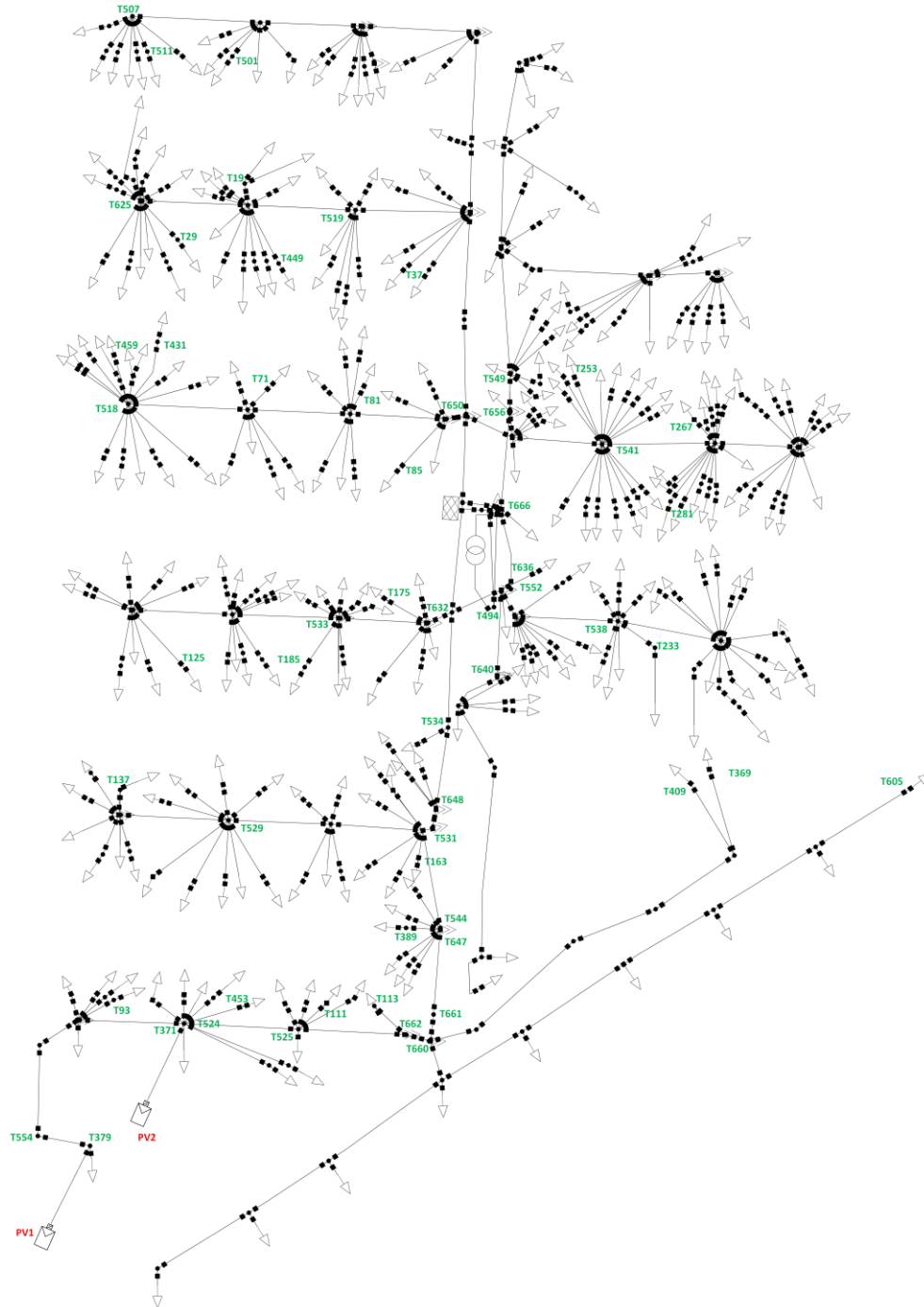


Fig. 7. Case study system

Firstly, the impact of considering harmonic current phase angle on  $THD_v$  and losses is evaluated. Fig. 8 displays box plots of  $THD_v$  for different buses without PVs. The top and bottom of each box are the 25<sup>th</sup> and 75<sup>th</sup> percentiles of the results, respectively. Also, the line in the middle of each box is the median. As can be seen in Fig. 8, considering phase angle as the real network condition decreases the  $THD_v$  compared to the situation without phase angle. When harmonic currents are modeled by both phase angle and magnitude, some harmonic currents may cancel out each other and thus, magnitude of harmonic current flowing throughout the network and consequently,  $THD_v$  is decreased. Due to the harmonic current magnitude reduction, total and harmonic losses for line and transformer are decreased as well (see Table III). This shows

the importance of considering phase angles in modeling harmonic currents. However, phase angles are ignored in many studies.

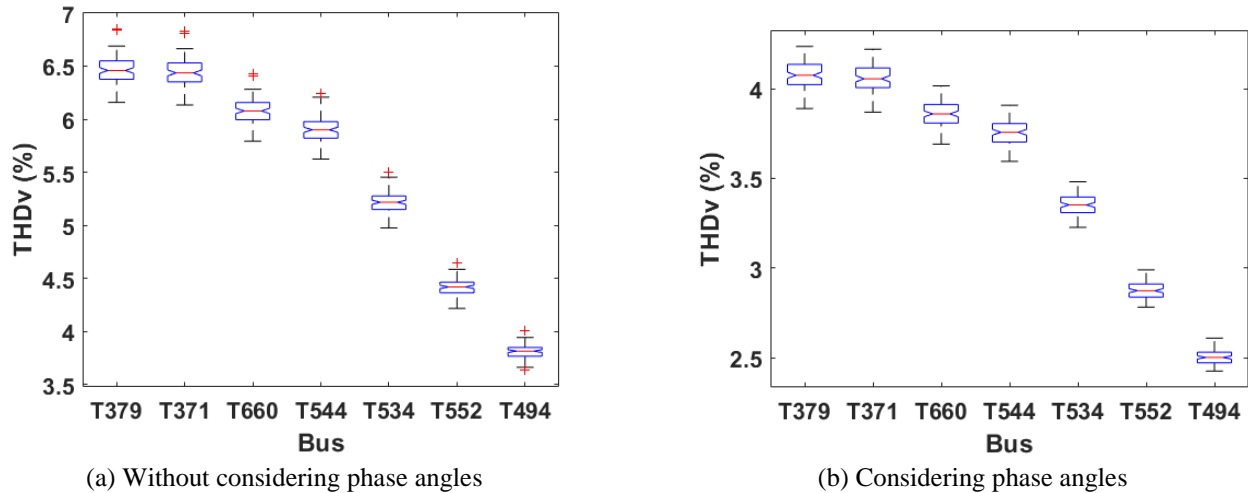


Fig. 8. Box plot of  $THD_v$  for some buses (rated power is considered as base value)

TABLE III  
Relation between phase angle and losses (rated power is considered as base value)

Case (without PV)	Harmonic losses (kW)	Total power losses (kW)	Harmonic losses (kW)	Total power losses (kW)
	Lines		Transformer	
Without considering phase angles	1.06028	14.8295	3.08661	12.6882
Considering phase angles	0.05445	13.8238	0.09056	9.6922

In Fig. 9, the active and reactive powers for each harmonic order are shown for the secondary side of transformer (for 80% PV penetration). It should be noted that fundamental frequency active and reactive powers are equal to 19.6 kW and 28 kVAr, respectively.

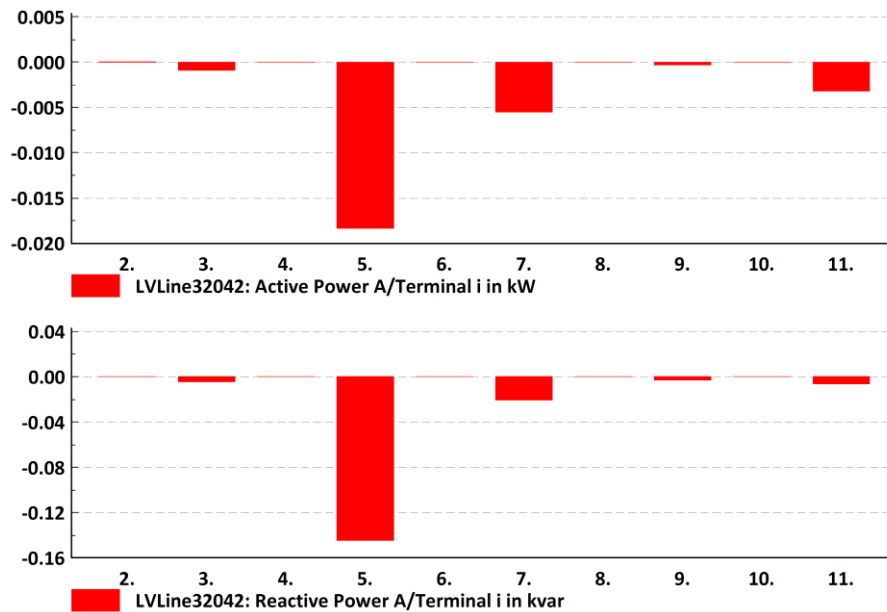


Fig. 9. Active and reactive powers for secondary side of transformer

Note that the current harmonic magnitudes of load and PV for orders 2-25 are relatively low and in addition, since phase angles of harmonic currents are also considered, some harmonic currents cancel each

other and thus, as can be seen in Fig. 9, the harmonic active and reactive powers are very low compared with the fundamental frequency powers. Therefore, with respect to these powers, the losses associated with harmonic orders are also very low.

It is noteworthy that network topology and characteristics such as loading conditions and length of distribution lines could affect the harmonic losses. For example, if the system loading is increased or length of lines are considered relatively longer in the test system, it can be clearly observed that the loss values increase. In this regard, please, see Table IV in which 80% PV penetration is assumed.

Fig. 10 shows the  $THD_v$  of some buses without and with different PV penetration rates.

TABLE IV  
Relation between power losses, load, and length of line

Case	Harmonic losses (kW)	Total power losses (kW)	Harmonic losses (kW)	Total power losses (kW)
	Lines		Transformer	
	<b>Present network</b>	0.10186	11.8598	0.13473
<b>Multiply load by 1.2</b>	0.15326	18.6686	0.20999	12.6605
<b>Multiply length of line by 4</b>	0.64779	70.1259	0.17399	11.5386
<b>Multiply length of line by 4 and load by 1.2</b>	1.08170	127.1628	0.31273	20.1047

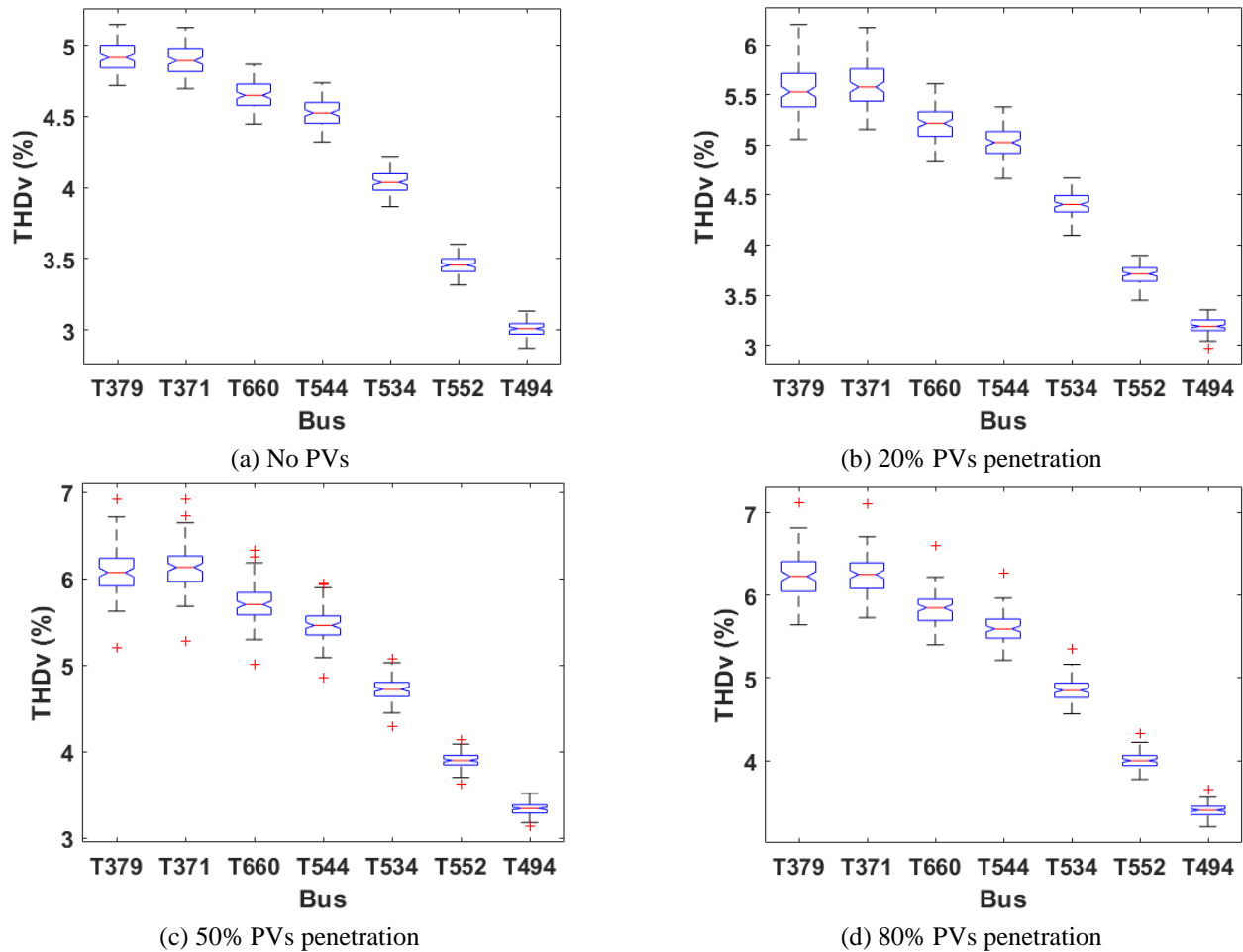


Fig. 10.  $THD_v$  of some buses (fundamental component is considered as base value)

Simulation results indicate that  $THD_v$  of buses increase as we get farther from the service transformer due to the nonlinear loads and harmonic currents injection by PVs. More importantly, by connecting more PVs to the network,  $THD_v$ s increase and go beyond the permissible ranges, but, the growth rate of  $THD_v$ s is

mitigated. Therefore, with increasing penetration of PVs, the network faces harmonic problems, which have to be addressed suitably. Here, optimal planning of PHFs is used as an effective solution to mitigate the mentioned issues. To this end, single-tuned PHFs with the quality factor ( $Q_p$ ) of 30 [35] are assumed to be optimally placed within the network. In Table V, the economic parameters used for simulations, including the value of  $Pr_m$ , number of operation years, and inflation and discount rates [55] are reported. Also,  $C_{act}$  [41],  $C_{fix_{cap}}$ ,  $C_{cap}$ , and  $C_{ind}$  are shown in this table [53].

TABLE V  
Economic parameters

$Pr_m$ (\$/kWh)	$N$ (year)	$ir$ (%)	$dr$ (%)	$C_{act}$ (\$/kW)	$C_{fix_{cap}}$ (\$)	$C_{cap}$ (\$/kVAr)	$C_{ind}$ (\$/kVAr)
0.06364	20	1.5	9	100	100	15	300

Based on the optimization results for 80% PV penetration, the optimal capacity ( $Q_{tot}$ ),  $Q_{rms_{cap}}$ ,  $Q_{rms_{ind}}$ , PHF cost, the harmonic tuning order, location of the three-phase star-connected PHFs, and Average RMS voltage of PHF location are determined as shown in Table VI. In Fig. 11, individual harmonic voltage distortions ( $HD_v$ ) and voltage waveform of T379 before and after planning are shown.

TABLE VI  
PHFs planning

Rated reactive power (kVAr)	$Q_{rms_{cap}}$ (kVAr)	$Q_{rms_{ind}}$ (kVAr)	PHF cost (\$)	Harmonic tuning order	Location	Average RMS voltage (pu)		
						Phase A	Phase B	Phase C
14	36.5	0.36	763.5	7	T371	0.97	0.92	0.93
77	80.6	7.07	3484.3	5	T632	0.97	0.96	0.95
39	14	0.82	562.8	15	T541	0.95	0.96	0.94
15	14	0.22	379.1	13	T519	0.94	0.95	0.93

As it can be seen in Fig. 11 (a), the odd orders have high values of  $HD_v$  before planning. By solving the proposed optimization problem, the fifth, seventh, thirteenth, and fifteenth harmonics are selected as the optimal harmonic tuning order of the planned PHF. In addition, since the 5<sup>th</sup> order has the maximum value of  $HD_v$  before planning, the highest cost and rated reactive power of PHFs (77 kVAr) is tuned for this order.

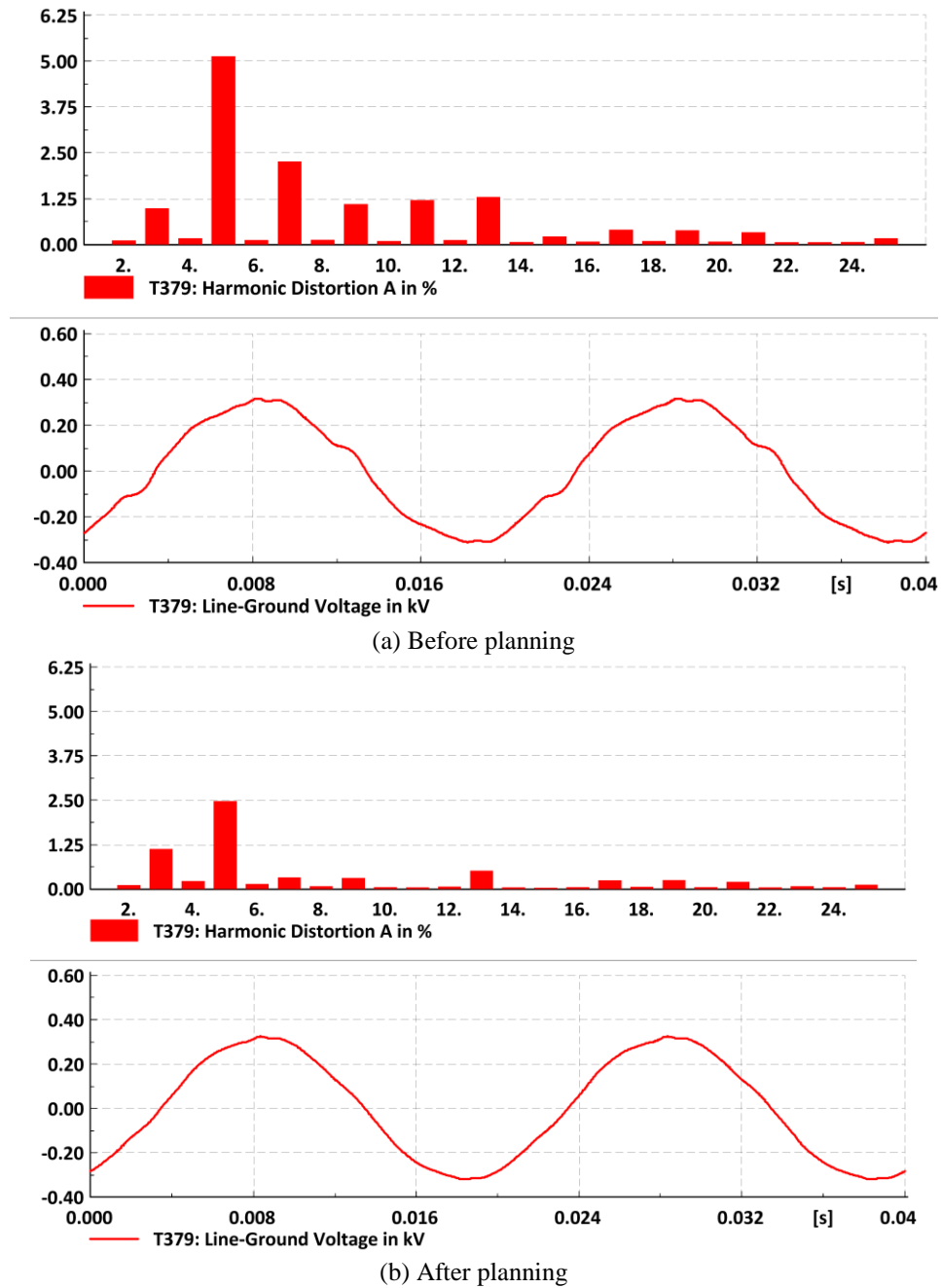
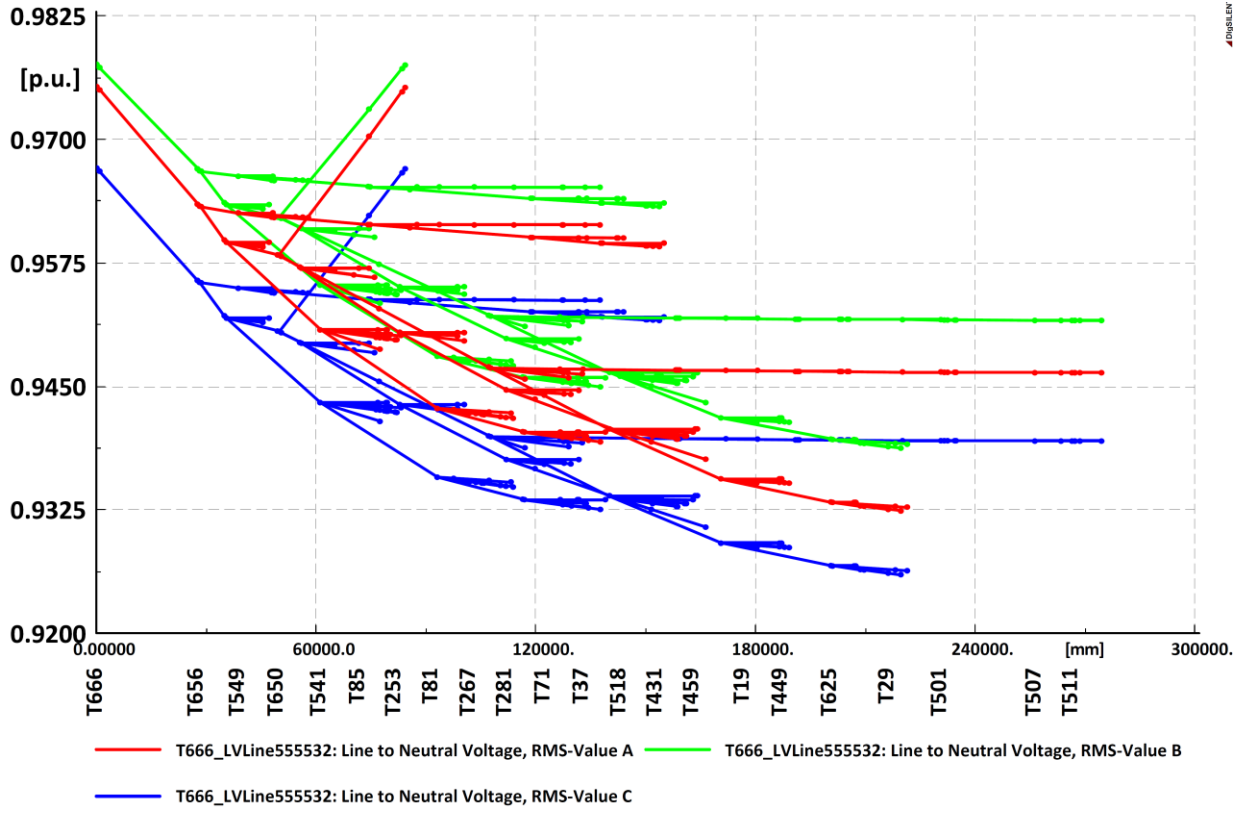


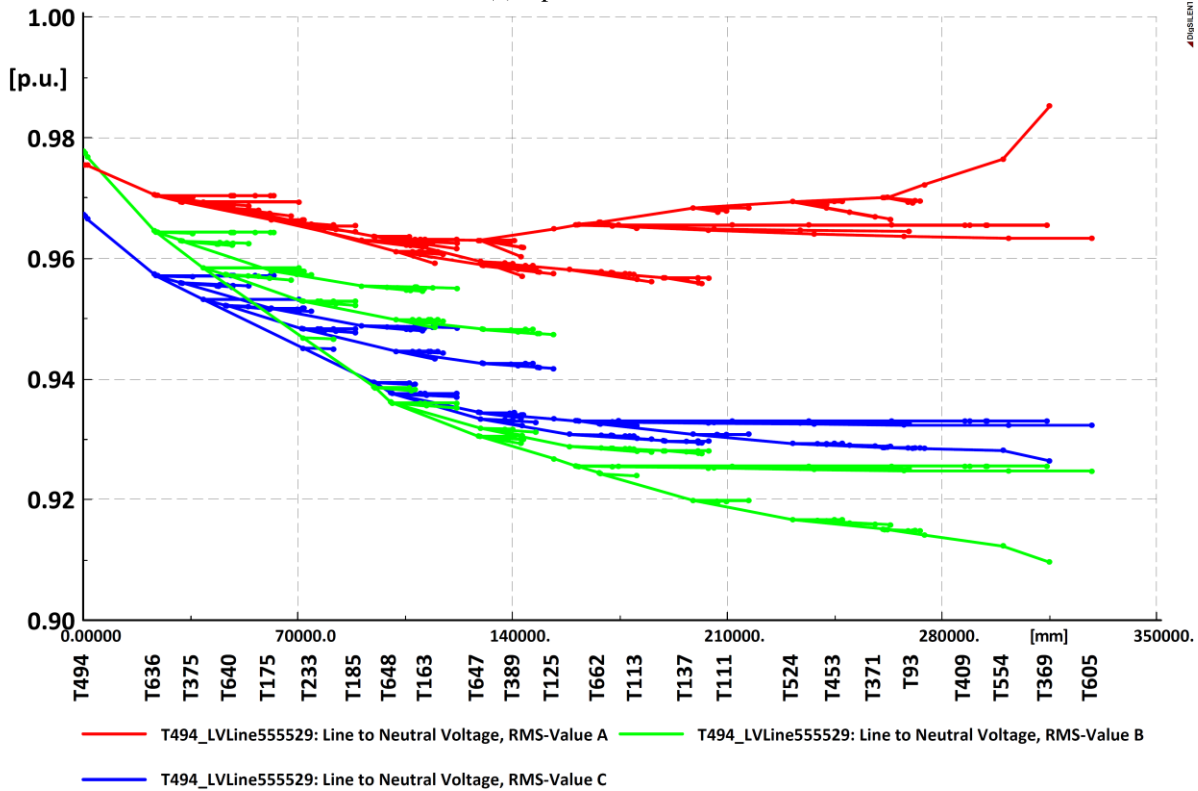
Fig. 11. Harmonic distortion for T379

As it can be understood in Fig. 11 (b), the 5<sup>th</sup>, 7<sup>th</sup>, 13<sup>th</sup>, and 15<sup>th</sup> orders HD<sub>v</sub> are decreased due to PHFs planning resulting to a better voltage quality.

To consider the worst case of harmonic, it is assumed that all loads are equal to their maximum power (full load). Adding PHFs to the network increase the voltage magnitude especially for the nearby buses. However, as can be seen in Table VI, due to heavy loading in this case study, the RMS voltages of PHF candidate buses do not exceed the allowable range after placing planned PHFs. As can be seen in Fig. 12 (voltage profile of upstream and downstream feeders for phases A, B, and C), by full loading (100%) and PHF planning, the RMS voltages of all buses are limited between 0.91 and 0.99. Therefore, RMS voltage constraint is satisfied.



(a) Upstream feeder



(b) Downstream feeder

Fig. 12. Voltage profile of feeders for phases A, B, and C in full (100%) load

Adding PHF to the case with low loading may increase voltage magnitude over allowable range. For very low loading condition, 20% loading is considered as worst case. For this situation, as can be seen in Fig. 13,

the RMS voltages of all buses are limited to  $\pm 10\%$  of nominal voltage.

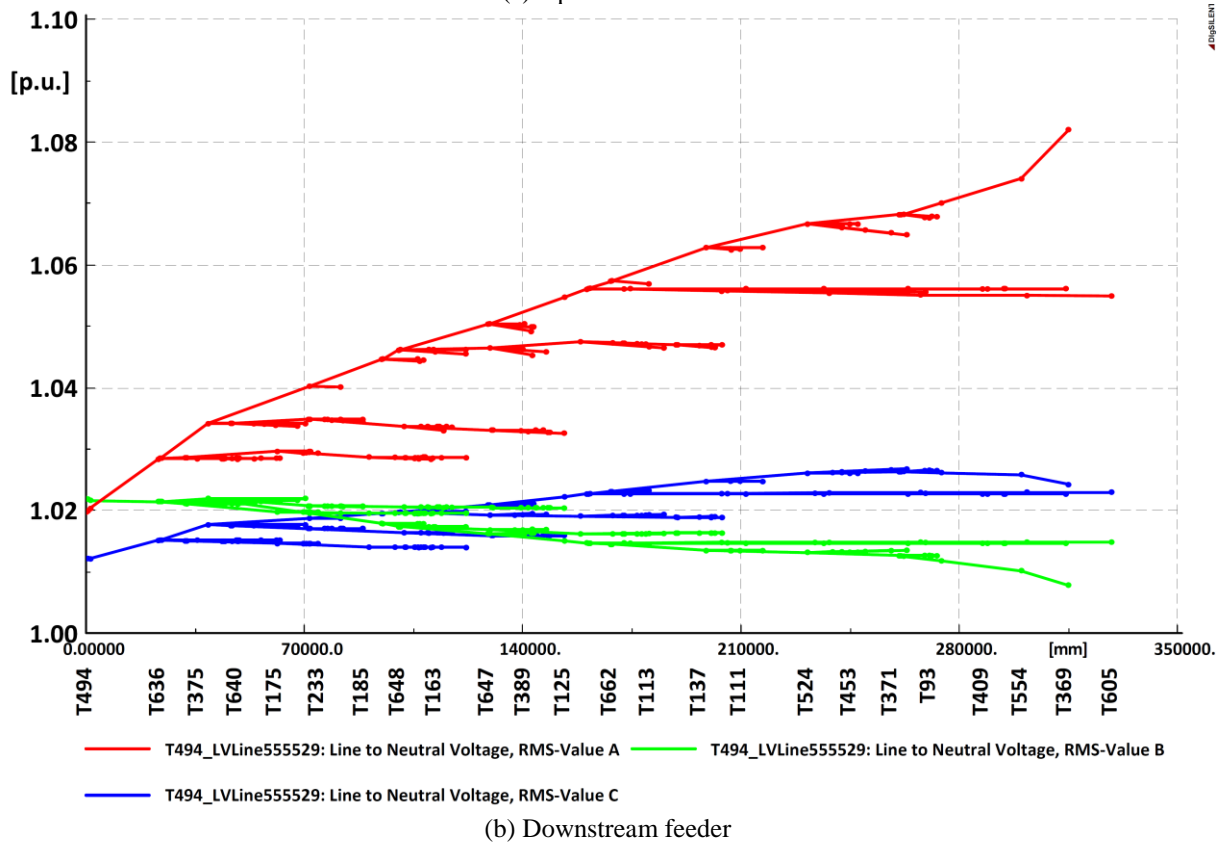
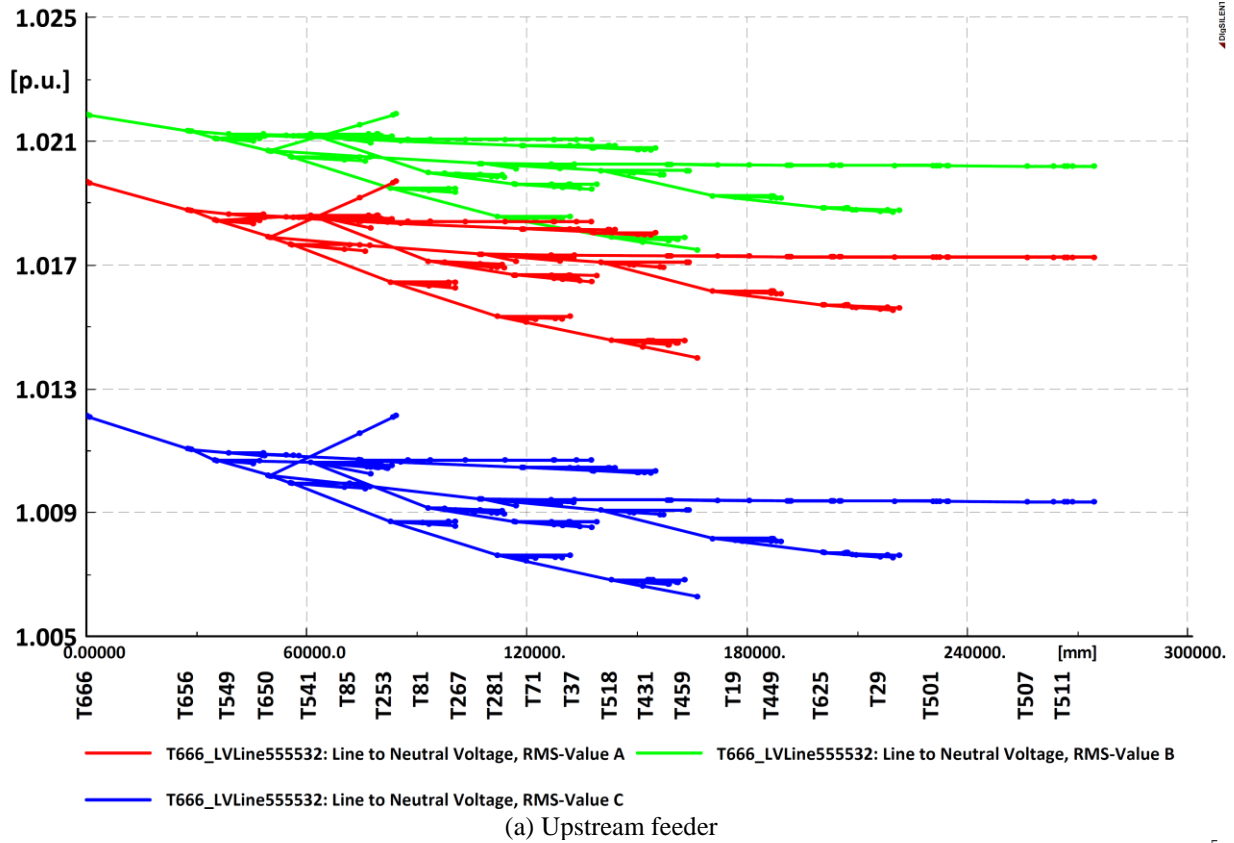


Fig. 13. Voltage profile of feeders for phases A, B, and C in 20% loading

In the present case, since all PV units are connected between phase A and neutral, RMS voltage of phase A is bigger than other phases for downstream feeder.

Table VII shows the average power losses for different phases of lines and transformer in various cases.

TABLE VII  
Average power losses in different cases

Case	Harmonic losses (kW)	Total power losses (kW)	Harmonic losses (kW)	Total power losses (kW)	Phase A losses (kW)	Phase B losses (kW)	Phase C losses (kW)
	Lines		Transformer		Lines		
<b>Without PV and PHF</b>	0.07953	13.8488	0.13142	9.7330	4.7779	4.4634	4.5280
<b>With 20% PVs penetration</b>	0.08756	13.4859	0.13620	9.5795	4.3898	4.5475	4.4610
<b>With 50% PVs penetration</b>	0.09710	12.7441	0.13399	8.9626	3.9804	4.4575	4.2092
<b>With 80% PVs penetration</b>	0.10186	11.8598	0.13473	8.1867	3.5511	4.2766	3.9303
<b>With 80% PVs penetration and PHF</b>	0.17713	9.8163	0.03735	6.2663	2.5728	3.8989	3.1675

According to Table VII, by increasing PVs penetration to 80%, harmonic losses (of lines) and total power losses (of lines and transformer) increase and decrease, respectively. Optimal PHF planning decreases total losses of lines and transformer. It should be noted that in DIGSILENT, only line losses can be divided into per-phase values.

According to Table VI, since  $THD_v$  values are higher for buses that are farther from the service transformer and especially the ones with PVs, T371 is proposed by the optimization algorithm as the candidate bus for PHF with rated reactive power equal to 14 kVAr. In addition, other PHFs are distributed in the network to decrease the losses.

This improvement in  $THD_v$  and losses is achieved at a net benefit of 17248.4 \$. In addition, increasing the allowable PV penetration, as a results of provided harmonic mitigation, can decrease environmental emission, increase the reliability, limit voltage drops experienced by end-consumers, and defer facility investment and construction of traditional power plants. Also, in summer, PV production matches with cooling load and thus, increases network stability. Therefore, with considering these advantages, mitigating harmonic effects of high PV penetration is very beneficial.

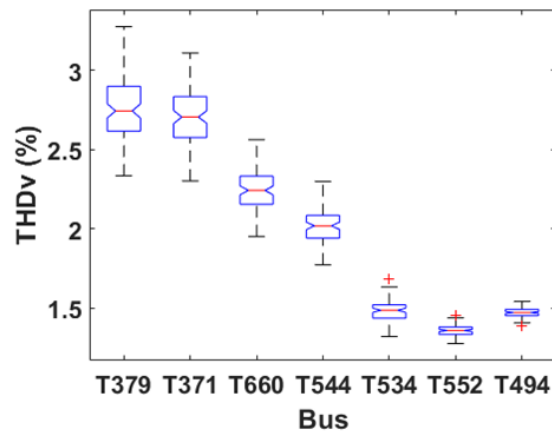
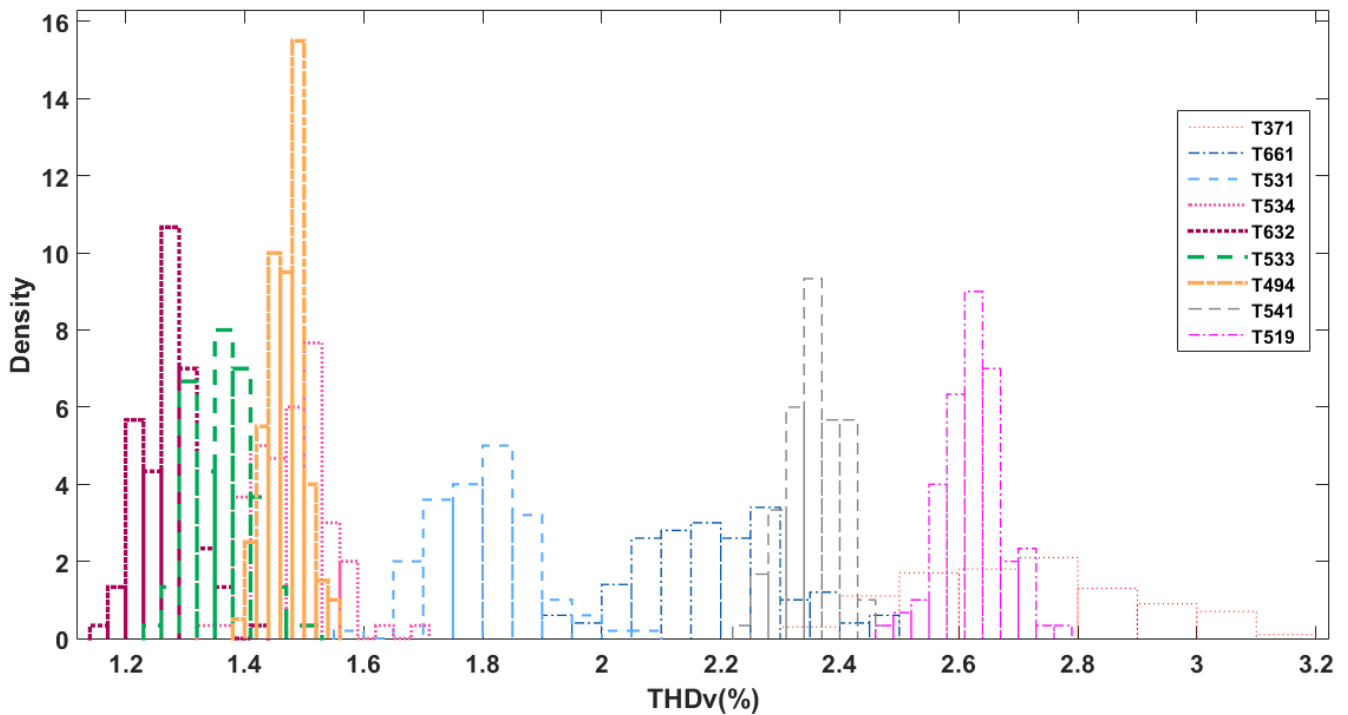
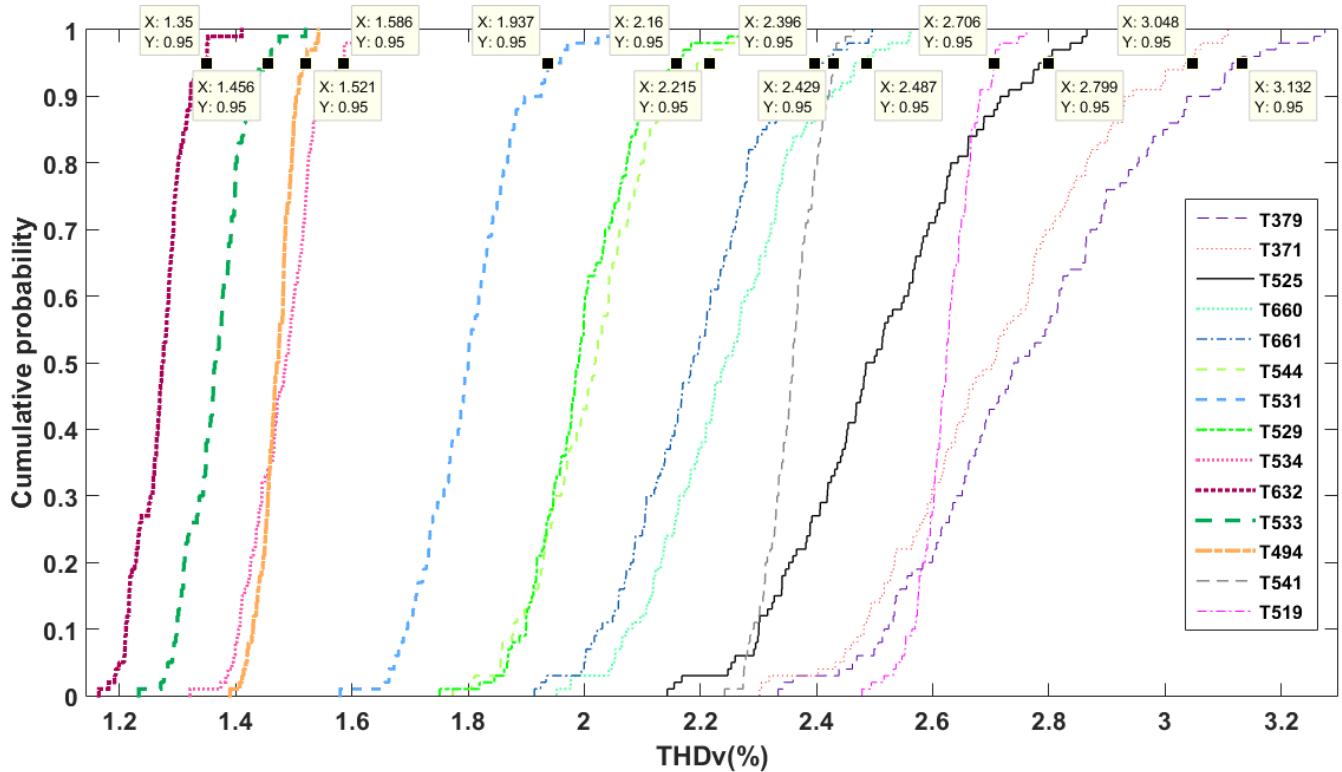


Fig. 14.  $THD_v$  after optimal planning of PHF for 80% PV penetration

Fig. 14 shows the  $THD_v$  values of buses by optimal planning of PHF for 80% PV penetration. As can be seen, due to PHFs planning, the  $THD_v$  of buses are limited under allowable range (5%).

Figs. 15 and 16 indicate PDF and CDF of  $THD_v$  for some buses after PHF planning for this PV penetration.

Fig. 15. PDF of  $THD_v$  for some busesFig. 16. CDF of  $THD_v$  for some buses

As can be seen from Fig. 15, PDF of  $THD_v$  for buses that are far from  $PV_s$  is similar to normal distribution because loads are modeled by normal PDF and  $PV_s$  are modeled according to measurements and a few of  $PV_s$  harmonic orders (i.e. only harmonic current magnitude of 5<sup>th</sup> order) are modeled by normal PDF (see Fig. 2). Also, for the buses which are near  $PV$  system, due to the different PDF of loads and  $PV_s$ , the PDF cannot be easily fitted by well-known distribution function. According to Fig. 16,  $THD_v$ s of buses T379, T531, and T494 are equal to 3.132%, 1.937%, and 1.521%, respectively, obtained by 95% cumulative

probability. According to economic objective function (6),  $THD_v$  of buses is maintained below 5% considering a 100% cumulative probability.

The rated reactive power, tuning order, and placement of three-phase star-connected PHFs are calculated to limit  $THD_v$  of phase A within the allowable range. By such PHFs,  $THD_v$  of phases B and C caused by nonlinear loads decrease, too.

Since the place of PV depends on consumers' requests and it is assumed that distribution network accepts the requests as much as possible, in this paper, a quasi-worst-case scenario (80%) is considered for optimal PHF planning. 80% penetration is a hypothetical case to guarantee if the penetrations of phases A, B and C are increased to 80% in the future, unacceptable harmonic conditions will not occur in such a network. PHF planning introduced in this paper is a general approach and can be applied for other practical cases, too (e.g., when single-phase PVs are almost evenly connected to all phases or three-phase PVs are added to distribution network).

In Fig. 17, the system frequency responses at T371, T632, T541, and T519 are shown. As it can be seen and also mentioned in [8], single-tuned PHF creates a parallel resonance point at a frequency below the tuned frequency. This resonant frequency must be safely away from main harmonics produced by the loads and PVs.

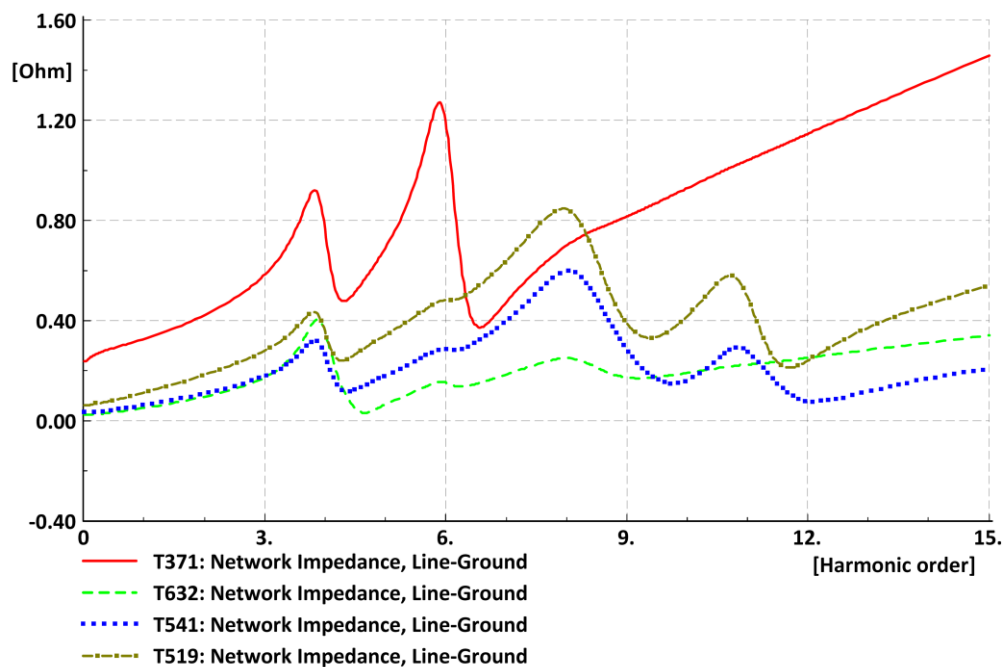


Fig. 17. System frequency response of T371, T632, T541, and T519

The convergence analysis of GA is performed, and the results are shown in Fig. 18. It can be seen that the used iteration number is enough because GA is converged within a number of iterations less than 30.

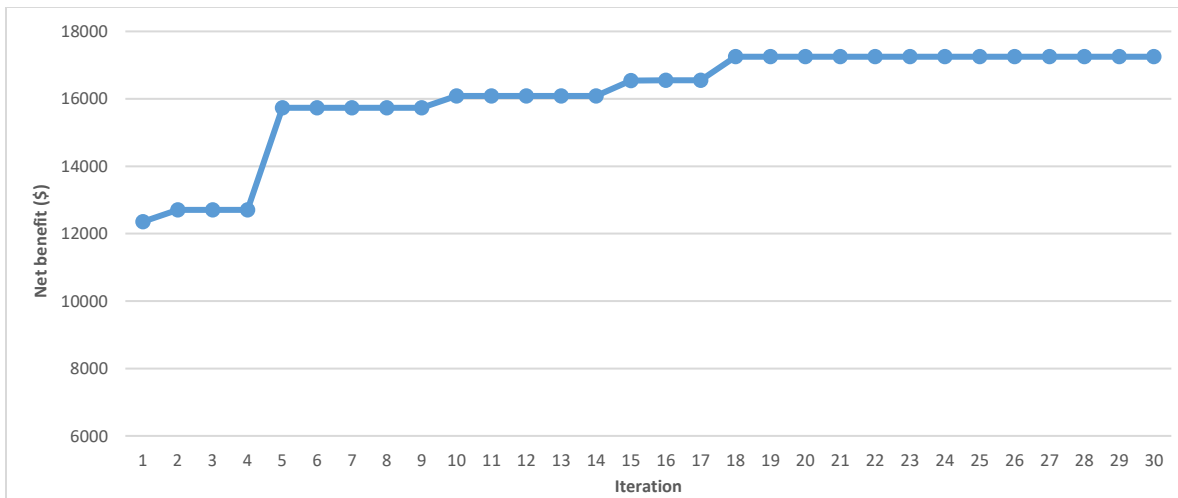


Fig. 18. Optimization process of GA

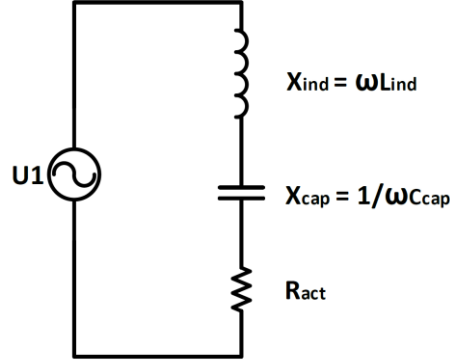
## V. CONCLUSION

This paper presented probabilistic optimization of PHFs considering real PV harmonic current and network data to mitigate harmonic impacts of PV and nonlinear loads. Due to the random nature of load and PV production, MCS was performed for probabilistic harmonic power flow. To increase the convergence rate of MCS while being computationally-efficient, the inverse-transform method was also applied for random variable generation. To increase the accuracy of results, the proposed method in this work considered both magnitude and phase angle of harmonic currents, frequency-dependent behavior of the network lines, and harmonic losses of the network. Also, the applicability and effectiveness of the proposed approach was tested and evaluated in a real distribution network using realistic information captured from the examined system.

Simulation results indicated that considering current phase angle in harmonic analysis (which denotes the real network condition), could result in lower  $THD_v$  values compared to situation where phase angle is neglected. It was also observed that  $THD_v$  of buses increases with distance from the service transformer and PDFs of  $THD_v$  for buses that are far from PV systems are very similar to a normal distribution. Furthermore, it is understood that by connecting more PVs to the network,  $THD_v$ s are increased. Results also indicated that by increasing the PV penetration to 80%, harmonic losses and total power losses increase and decrease, respectively. Numerical results demonstrated also that by optimal PHF planning,  $THD_v$ s of all buses could be kept within the allowable limits and total losses could be decreased.

It should be mentioned that since the modeling approach in this paper is based on measurement, harmonic interactions between nonlinear loads and PV systems have not been taken into account; thus, it is worthy to address this issue in future studies.

## VI. APPENDIX



By defining  $Q_{ind}$  and  $Q_{cap}$  as following

$$Q_{ind} \triangleq \frac{U_1^2}{X_{ind}} = \frac{U_1^2}{\omega L_{ind}} = \frac{U_1^2}{2\pi f_1 L_{ind}}$$

$$Q_{cap} \triangleq \frac{U_1^2}{X_{cap}} = U_1^2 (\omega C_{cap}) = U_1^2 (2\pi f_1 C_{cap})$$

$$\begin{aligned} \text{In resonance: } (X_{ind})_{res} &= (X_{cap})_{res} \rightarrow 2\pi f_{res} L_{ind} = \frac{1}{2\pi f_{res} C_{cap}} \rightarrow 2\pi n_{res} f_1 L_{ind} = \frac{1}{2\pi n_{res} f_1 C_{cap}} \\ &\rightarrow X_{ind} = \frac{X_{cap}}{n_{res}^2} \end{aligned}$$

$$\begin{aligned} Q_{tot} &= \frac{U_1^2}{X_{cap} - X_{ind}} = \frac{U_1^2}{X_{cap} - \frac{X_{cap}}{n_{res}^2}} = \frac{U_1^2}{X_{cap} \left(1 - \frac{1}{n_{res}^2}\right)} = \frac{Q_{cap}}{\left(1 - \frac{1}{n_{res}^2}\right)} \\ &\rightarrow Q_{cap} = Q_{tot} \left(1 - \frac{1}{n_{res}^2}\right) \end{aligned}$$

$$\begin{aligned} Q_{tot} &= \frac{U_1^2}{X_{cap} - X_{ind}} = \frac{U_1^2}{n_{res}^2 X_{ind} - X_{ind}} = \frac{U_1^2}{X_{ind} (n_{res}^2 - 1)} = \frac{Q_{ind}}{(n_{res}^2 - 1)} \\ &\rightarrow Q_{ind} = Q_{tot} (n_{res}^2 - 1) \end{aligned}$$

## REFERENCES

- [1] K. Padmanathan, U. Govindarajan, V. K. Ramachandaramurthy, S. O. Selvi T, and B. Jeevarathinam, "Integrating solar photovoltaic energy conversion systems into industrial and commercial electrical energy utilization—A survey," *J. Ind. Inf. Integr.*, vol. 10, pp. 39-54, Jun. 2018.
- [2] A. Kalair, N. Abas, A. R. Kalair, Z. Saleem, and N. Khan, "Review of harmonic analysis, modeling and mitigation techniques," *Renewable Sustain. Energy Rev.*, vol. 78, pp. 1152-1187, Oct. 2017.
- [3] O. S. Nduka and B. C. Pal, "Quantitative evaluation of actual loss reduction benefits of a renewable heavy DG distribution network," *IEEE Trans. Sustain. Energy*, vol. 9, no. 3, pp. 1384-1396, Jul. 2018.
- [4] H. Hu, Q. Shi, Z. He, J. He, and S. Gao, "Potential harmonic resonance impacts of PV inverter filters on distribution systems," *IEEE Trans. Sustain. Energy*, vol. 6, no. 1, pp. 151-161, Jan. 2015.

- [5] Sh. Wang, X. Liu, K. Wang, L. Wu, and Y. Zhang, "Tracing harmonic contributions of multiple distributed generations in distribution systems with uncertainty," *Int. J. Elect. Power Energy Syst.*, vol. 95, pp. 585-591, Feb. 2018.
- [6] S. S. Kaddah, Kh. M. Abo-Al-Ez, T. F. Megahed, and M. G. Osman, "Probabilistic power quality indices for electric grids with increased penetration level of wind power generation," *Int. J. Elect. Power Energy Syst.*, vol. 77, pp. 50-58, May 2016.
- [7] S. Sakar, M. E. Balci, Sh. H. E. A. Aleem, and A. F. Zobaa, "Increasing PV hosting capacity in distorted distribution systems using passive harmonic filtering," *Elect. Power Syst. Res.*, vol. 148, pp. 74-86, Jul. 2017.
- [8] R. C. Dugan, M. F. McGranaghan, S. Santoso, and H. W. Beaty, "Applied Harmonics," in *Electrical Power Systems Quality*, 2nd ed., McGraw-Hill Education, 2004, ch. 6, pp. 225-294.
- [9] H. Akagi, "New trends in active filters for power conditioning," *IEEE Trans. Ind. Appl.*, vol. 32, no. 6, pp. 1312-1322, Nov/Dec 1996.
- [10] Y. Y. Hong, Ch. Sh. Chiu, and Sh. W. Huang, "Multi-scenario passive filter planning in factory distribution system by using Markov model and probabilistic Sugeno fuzzy reasoning," *Appl. Soft Comput.*, vol. 41, pp. 352-361, Apr. 2016.
- [11] S. Sakar, M. E. Balci, Sh. H. E. A. Aleem, and A. F. Zobaa, "Integration of large- scale PV plants in non-sinusoidal environments: Considerations on hosting capacity and harmonic distortion limits Review article," *Renewable Sustain. Energy Rev.*, vol. 82, pp. 176-186, Feb. 2018.
- [12] Y. L. Chen, "Optimal multi-objective single-tuned harmonic filter planning," *IEEE Trans. Power Del.*, vol. 20, no. 2, pp. 1191-1197, Apr. 2005.
- [13] Y. P. Chang and Ch. Low, "Optimization of a passive harmonic filter based on the neural-genetic algorithm with fuzzy logic for a steel manufacturing plant," *Expert Syst. Appl.*, vol. 34, no. 3, pp. 2059-2070, Apr. 2008.
- [14] Y. P. Chang, "Integration of SQP and PSO for optimal planning of harmonic filters," *Expert Syst. Appl.*, vol. 37, no. 3, pp. 2522-2530, Mar. 2010.
- [15] G. W. Chang, S. Y. Chu, and H. L. Wang, "A new method of passive harmonic filter planning for controlling voltage distortion in a power system," *IEEE Trans. Power Del.*, vol. 21, no. 1, pp. 305-312, Jan. 2006.
- [16] M. Mohammadi, "Bacterial foraging optimization and adaptive version for economically optimum sitting, sizing and harmonic tuning orders setting of LC harmonic passive power filters in radial distribution systems with linear and nonlinear loads," *Appl. Soft Comput.*, vol. 29, pp. 345-356, Apr. 2015.
- [17] M. Mohammadi, A. M. Rozbahani, and M. Montazeri, "Multi criteria simultaneous planning of passive filters and distributed generation simultaneously in distribution system considering nonlinear loads with adaptive bacterial foraging optimization approach," *Int. J. Elect. Power Energy Syst.*, vol. 79, pp. 253-262, Jul. 2016.
- [18] N. H. B. A. Kahar, and A. F. Zobaa, "Application of mixed integer distributed ant colony optimization to the design of undamped single-tuned passive filters based harmonics mitigation," *Swarm Evol. Comput.*, to be published. doi: 10.1016/j.swevo.2018.03.004.
- [19] J. C. Leite, I. P. Abril, and M. S. S. Azevedo, "Capacitor and passive filter placement in distribution systems by nondominated sorting genetic algorithm-II," *Elect. Power Syst. Res.*, vol. 143, pp. 482-489, Feb. 2017.
- [20] N. Yang and M. Le, "Optimal design of passive power filters based on multi-objective bat algorithm and pareto front," *Appl. Soft Comput.*, vol. 35, pp. 257-266, Oct. 2015.
- [21] N. Yang and M. Le, "Multi-objective bat algorithm with time-varying inertia weights for optimal design of passive power filters set," *IET Gener., Transmiss. Distrib.*, vol. 9, no. 7, pp. 644-654, Apr. 2015.
- [22] A. Karadeniz and M. E. Balci, "Comparative evaluation of common passive filter types regarding maximization of transformer's loading capability under non-sinusoidal conditions," *Elect. Power Syst. Res.*, vol. 185, pp. 324-334, May 2018.
- [23] Sh. H. E. A. Aleem, M. E. Balci, and S. Sakar, "Effective utilization of cables and transformers using passive filters for non-linear loads," *Int. J. Elect. Power Energy Syst.*, vol. 71, pp. 344-350, Oct. 2015.
- [24] K. Abolfathi, M. Babaei, and A. Ahmarinejad, "Designing optimal passive filters for transformers under harmonic conditions," in *4th Int. Conf. Power Energy Syst. Eng. (CPESE 2017)*, Berlin, 2017, PP. 411-417.
- [25] G. W. Chang, H. L. Wang, and S. Y. Chu, "A probabilistic approach for optimal passive harmonic filter planning," *IEEE Trans. Power Del.*, vol. 22, no. 3, pp. 1790-1798, Jul. 2007.
- [26] G. W. Chang, H. L. Wang, and S. Y. Chu, "Probabilistic approach for passive harmonic filter planning in a power system," in *2006 Int. Conf. Power Syst. Technol.*, Chongqing, 2006, pp. 1-5.
- [27] G. W. Chang, H. L. Wang, G. S. Chuang, and S. Y. Chu, "Passive harmonic filter planning in a power system with considering probabilistic constraints," *IEEE Trans. Power Del.*, vol. 24, no. 1, pp. 208-218, Jan. 2009.
- [28] G. Carpinelli, G. Ferruzzi, and A. Russo, "A heuristic multi-objective approach with trade off/risk analysis issues for passive harmonic filters planning I. Problem formulation and solution algorithm," in *8th Mediter. Conf. on Power Gener., Transmiss., Distrib. and Energy Convers. (MEDPOWER 2012)*, Cagliari, 2012, pp. 1-8.

- [29] Y. Y. Hong and Ch. Sh. Chiu, "Passive filter planning using simultaneous perturbation stochastic approximation," *IEEE Trans. Power Del.*, vol. 25, no. 2, pp. 939-946, Apr. 2010.
- [30] Y. Y. Hong and W. J. Liao, "Optimal passive filter planning considering probabilistic parameters using cumulant and adaptive dynamic clone selection algorithm," *Int. J. Elect. Power Energy Syst.*, vol. 45, no. 1, pp. 159-166, Feb. 2013.
- [31] Y. P. Chang, W. K. Tseng, and T. F. Tsao, "Application of combined feasible-direction method and genetic algorithm to optimal planning of harmonic filters considering uncertainty conditions," *IEE Proc. Gener., Transmiss. Distrib.*, vol. 152, no. 5, pp. 729-736, Sep. 2005.
- [32] Y. P. Chang and Ch. J. Wu, "Optimal multiobjective planning of large-scale passive harmonic filters using hybrid differential evolution method considering parameter and loading uncertainty," *IEEE Trans. Power Del.*, vol. 20, no. 1, pp. 408-416, Jan. 2005.
- [33] Z. Li, H. Hu, Y. Wang, L. Tang, Z. He, and S. Gao, "Probabilistic harmonic resonance assessment considering power system uncertainties," *IEEE Trans. Power Del.*, to be published. doi: 10.1109/TPWRD.2018.2846608.
- [34] Y. P. Chang, Ch. Low, and Ch. J. Wu, "Optimal design of discrete-value passive harmonic filters using sequential neural-network approximation and orthogonal array," *IEEE Trans. Power Del.*, vol. 22, no. 3, pp. 1813-1821, Jul. 2007.
- [35] Y. P. Chang, Ch. Low, and Sh. Y. Hung, "Integrated feasible direction method and genetic algorithm for optimal planning of harmonic filters with uncertainty conditions," *Expert Syst. Appl.*, vol. 36, no. 2, pp. 3946-3955, Mar. 2009.
- [36] P. Bagheri, W. Xu, and T. Ding, "A distributed filtering scheme to mitigate harmonics in residential distribution systems," *IEEE Trans. Power Del.*, vol. 31, no. 2, pp. 648-656, Apr. 2016.
- [37] H. A. M. Ali, A. F. Zobaa, and E. E. A. El-Zahab, "Single-tuned passive harmonic filters design with uncertain source and load characteristics," *Rec. Pate. on Elect. Eng.*, vol. 5, no. 1, pp. 72-80, Apr. 2012.
- [38] G. Carpinelli, G. Ferruzzi, and A. Russo, "Trade-off analysis to solve a probabilistic multi-objective problem for passive filtering system planning," *Int. J. Emerg. Elect. Power Syst.*, vol. 14, no. 3, pp. 2194-5756, May 2013.
- [39] Y. Zhao, H. Deng, J. Li, and D. Xia, "Optimal planning of harmonic filters on distribution systems by chance constrained programming," *Elect. Power Syst. Res.*, vol. 68, no. 2, pp. 149-156, Feb. 2004.
- [40] Ch. f. Yang, G. G. Lai, and Ch. T. Su, "Optimal planning of passive harmonic filters using hybrid differential evolution considering variation of system parameters," *Int. Trans. Elect. Energy Syst.*, vol. 23, no. 8, pp. 1317-1334, Nov. 2013.
- [41] M. M. Elkholy, M. A. El-Hameed, and A. A. El-Fergany, "Harmonic analysis of hybrid renewable microgrids comprising optimal design of passive filters and uncertainties," *Elect. Power Syst. Res.*, vol. 163, no. Part A, pp. 491-501, Oct. 2018.
- [42] *Technical reference documentation: filter/shunt*, power factory Co., Germany, 2018.
- [43] J. Wasilewski, W. Wiechowski, and C. L. Bak, "Harmonic domain modeling of a distribution system using the DIgSILENT PowerFactory software," in *2005 Int. Conf. Futu. Power Syst.*, Amsterdam, 2005, pp. 1-7.
- [44] O. S. Nduka and B. C. Pal, "Harmonic domain modeling of PV system for the assessment of grid integration impact," *IEEE Trans. Sustain. Energy*, vol. 8, no. 3, pp. 1154-1165, 2017.
- [45] M. Gomez-Gonzalez, F. J. Ruiz-Rodriguez, and F. Jurado, "A binary SFLA for probabilistic three-phase load flow in unbalanced distribution systems with technical constraints," *Int. J. Elect. Power Energy Syst.*, vol. 48, pp. 48-57, Jun. 2013.
- [46] G. Carpinelli, P. Caramia, and P. Varilone, "Multi-linear Monte Carlo simulation method for probabilistic load flow of distribution systems with wind and photovoltaic generation systems," *Renewable Energy*, vol. 76, pp. 283-295, Apr. 2015.
- [47] A. A. Abdelsalam and E. F. El-Saadany, "Probabilistic approach for optimal planning of distributed generators with controlling harmonic distortions," *IET Gener., Transmiss. Distrib.*, vol. 7, no. 10, pp. 1105-1115, Oct. 2013.
- [48] S. Conti and S. Raiti, "Probabilistic load flow using Monte Carlo techniques for distribution networks with photovoltaic generators," *Solar Energy*, vol. 81, no. 12, pp. 1473-1481, Dec. 2007.
- [49] R. Y. Rubinstein and D. P. Kroese, "Random number, random variable, and stochastic process generation," in *Simulation and the Monte Carlo Method*, 2nd ed., wiley, 2007, ch. 2, pp. 49-80.
- [50] M. N. Kabir, Y. Mishra, and R. C. Bansal, "Probabilistic load flow for distribution systems with uncertain PV generation," *Applied Energy*, vol. 163, pp. 343-351, Feb. 2016.
- [51] *IEEE draft guide for applying harmonic limits on power systems*, IEEE P519.1/D12, 2015.
- [52] F. M. G. Longatt and J. L. R. Torres, "Probabilistic power flow module for powerfactory DIgSILENT," in *PowerFactory Applications for Power System Analysis*, springer, 2014, ch. 3, pp. 61-84.
- [53] C. Kawann and A. E. Emanuel, "Passive shunt harmonic filters for low and medium voltage: a cost comparison study," *IEEE Trans. Power Syst.*, vol. 11, no. 4, pp. 1825-1831, Nov. 1996.
- [54] *Compatibility levels for low frequency conducted disturbances and signalling in public low voltage power supply systems*, IEC 61000-2-2, 1990.

- [55] R. C. Leou, "An economic analysis model for the energy storage system applied to a distribution substation," *Int. J. Elect. Power Energy Syst.*, vol. 34, no. 1, pp. 132-137, Jan. 2012.